Elastic and rotational excitation of the hydrogen molecule by 1–200-eV positron impact

P. K. Bhattacharyya and D. K. Syamal
Department of Physics, Calcutta University, 92 Acharya Prafulla Chandra Road, Calcutta 700009, West Bengal, India
(Received 17 November 1982; revised manuscript received 20 May 1983)

Pure elastic scattering ($J=0\rightarrow J'=0$ and $J=1\rightarrow J'=1$), rotational excitation ($J=0\rightarrow J'=2$ and $J=1\rightarrow J'=3$), and average elastic (pure elastic plus rotational excitation) cross sections of the hydrogen molecule by 1–200-eV positrons are computed by using the adiabatic approximation in which the Glauber-type eikonal amplitude for a fixed molecular orientation is considered as input. Both differential and total scattering cross sections are calculated. Momentum-transfer cross sections are also obtained. Two different model effective potentials for positron–hydrogen-molecule interactions have been considered. Effects of positronium formation channel are neglected. Comparison is made with the recent measurements as well as with the available theoretical calculations. Below the positronium formation threshold average total elastic-scattering cross sections are found to reproduce the experimental data quite accurately. Electron and positron scattering cross sections at intermediate energies are compared. The effects of polarization interaction are found to be significant even at 200 eV.

I. INTRODUCTION

In recent years, the problem of scattering of positrons by atoms and molecules has received considerable attention.[1–8] Positron scattering differs in many respects from electron scattering. First, in positron scattering the Pauli exclusion principle, which gives rise to exchange interaction in electron scattering, does not come into play. Second, the effects of polarization and static potentials tend to cancel each other for positrons, but they are additive for electrons. Thus, the scattering cross sections involving positrons depend sensitively on the degree of cancellation of these two effects in the energy region where the distortion of the target cannot be neglected. Third, the formation of positronium and free annihilation are two new inelastic processes which occur only for positrons. Because of these basic differences between positron and electron scattering the study of positron scattering is expected to provide a better understanding of the scattering phenomenon. For example, the second aspect of positron scattering mentioned above can be utilized to assess the relative importance of polarization interaction arising from the distortion of the target by the projectile. In fact, the accuracy, applicability, and superiority of a particular approximation over others used in electron scattering can be tested by carefully applying these approximations to positron scattering and by comparing the results so obtained with the corresponding results computed for electron scattering. For this, reliable experimental data for positron-atom(molecule) scattering are needed. During the last few years considerable attempts have been made[2–5] in this direction. As a result, more and more accurate positron scattering data for some atoms[2–5,9] and molecules[2–5,10,11] are now being reported from different laboratories.

Theoretically, the problem of positron-molecule scattering poses greater difficulties, compared to that of positron-atom scattering, because of the multicenter nature of the problem. Amongst the molecular targets,[7,8,12] the hydrogen molecule[12–18] was studied most. Lodge *et al.*[13] studied the elastic scattering of low-energy positrons by hydrogen molecules using the adiabatic-nuclei approximation. Their work was extended by Baille *et al.*[14] to include the rotational excitation of the hydrogen molecule. Hara[15] performed similar calculations using the two-center formalism. The rotational-excitation cross sections were computed earlier by Hara[12] using the distorted-wave approximation. A comparative study of the average elastic- (rotationally summed) scattering and rotational-excitation cross sections obtained by using the one-center and two-center expansions of the effective positron–hydrogen-molecule potential was made by Darewych *et al.*[16] Bhattacharyya and Ghosh[17] applied the Glauber-type eikonal approximation to compute average elastic-scattering cross sections up to an incident positron energy of 50 eV. Recently, Sur and Ghosh[18] calculated the low-energy average elastic cross sections by using the two-center formalism following Hara.[19] Amongst these calculations, the results of Bhattacharyya and Ghosh were found to give the best fit to experimental total scattering cross sections below the positronium formation threshold. But these authors treated the averaging of the cross sections over molecular orientations in an unsatisfactory way. In the present investigation we have eliminated this shortcoming in the computation of average total elastic-scattering cross sections following the procedure proposed by Bhattacharyya and Ghosh[20] and applied successfully to electron scattering by homonuclear diatomic molecules.[21–23] It will be interesting to see how these cross sections agree with the more accurate experimental data now available[11] in the literature. Moreover, we have calculated in the present paper pure elastic-scattering and rotational-excitation cross sections using the adiabatic approximation. The calculations are made over a wider range in positron energy, namely, 1–200 eV. Finally, positron and electron cross sections at intermediate energies

are compared in detail to investigate the role of positrons and electrons as projectiles.

II. EFFECTIVE POTENTIAL AND THEORY

The effective positron–hydrogen-molecule potential $V(\vec{r},\hat{R})$, neglecting the positronium formation channel, can be written as

$$V(\vec{r},\hat{R})=V_s(\vec{r},\hat{R})+V_p(\vec{r},\hat{R}) , \tag{1}$$

where $V_s(\vec{r},\hat{R})$ represents the electrostatic interaction between the positron and the undistorted ground-electronic charge distribution of the molecule and $V_p(\vec{r},\hat{R})$ is the polarization potential representing the effects of the distortion of the target. $\hat{R}$ is the unit vector along $\vec{R}$, where R is the equilibrium internuclear separation and $\vec{r}$ is the position vector of the scattered positron measured from the center of mass of the molecule. We expand $V(\vec{r},\hat{R})$ in terms of Legendre polynomials:

$$V(\vec{r},\hat{R})=\sum_{\nu=0} V^{\nu}(r)P_{\nu}(\hat{r}\cdot\hat{R}) . \tag{2}$$

For homonuclear diatomic molecules only even values of ν, including zero, are included in the summation. Because of the slow convergence of the expression (2) near the nuclei, a large number of terms are required to represent properly the effective potential $V(\vec{r},\hat{R})$. For the hydrogen molecule, however, we can neglect, to a good approximation, terms higher than $\nu=2$. Thus using the expression (2) in (1) the first two nonvanishing Legendre coefficients become

$$V^0(r)=V_s^0(r)+V_p^0(r) , \tag{3}$$

$$V^2(r)=V_s^2(r)+V_p^2(r) ,$$

in which $V_s^2(r)$, $V_p^0(r)$, and $V_p^2(r)$ should behave, at large r, as

$$V_s^2(r)\underset{r\to\infty}{\sim}-Q/r^3,\quad V_p^0(r)\underset{r\to\infty}{\sim}-\alpha_0/2r^4 ,$$
and
$$V_p^2(r)\underset{r\to\infty}{\sim}-\alpha_2/2r^4 , \tag{4}$$

where Q, α_0, and α_2 are, respectively, the quadrupole moment and the spherical and nonspherical parts of the static dipole polarizability. In this paper we have used the Wang wave function[24] to calculate $V_s^0(r)$ and $V_s^2(r)$, the explicit expressions of which were reported in Ref. 25. $V_s^2(r)$ so obtained, we call this $V_s^{2W}(r)$, does not reproduce the quadrupole tail properly. For that reason we have modified $V_s^{2W}(r)$ with a term $V_q^2(r)$ such that the asymptotic behavior of $V_s^2(r)$ is well represented:

$$V_s^2(r)=V_s^{2W}(r)+V_q^2(r) . \tag{5}$$

Furthermore, the small-r behavior of the long-range potentials $V_p^0(r)$ and $V_p^2(r)$ is not known accurately. A few calculations of these potentials are available in the literature for simple molecules.[26] In general, a cutoff function with some adjustable parameter is used[19,27] to make these potentials well behaved at the center of mass of the molecule, while the calculated cross sections are made to agree with the experimental results. In the present investigation the following two forms[7] are considered for $V_q^2(r)$, $V_p^0(r)$, and $V_p^2(r)$.

Model A. We have

$$V_q^2(r)=-Qr^3(r^2+r_0^2)^{-3} ,$$
$$V_p^0(r)=-\tfrac{1}{2}\alpha_0(r^2+r_0^2)^{-2} ,$$
$$V_p^2(r)=-\tfrac{1}{2}\alpha_2 r^2(r^2+r_0^2)^{-3} ,$$

where the cutoff parameter $r_0=1.6a_0$.

Model B. We have

$$V_q^2(r)=-Qr^{-3}(1-e^{-(r/r_c)^6}) ,$$
$$V_p^0(r)=-\tfrac{1}{2}\alpha_0(r^2+R_1^2)^{-2}(1-e^{-(r/R_a)^3}) ,$$
$$V_p^2(r)=\begin{cases}-\tfrac{1}{2}\alpha_2(r^2-R_2^2)^{-2}(1-e^{-(r/R_b)^4}), & r\geq 0.5a_0\\ 0, & r<0.5a_0\end{cases}$$

where $R_1=1.22a_0$, $R_2=0.1a_0$, $R_a=1.7a_0$, $R_b=2a_0$, and $r_c=1.8a_0$.

It is to be noted that model A was suggested by Hara[19] by matching the low-energy theoretical cross sections (e^--H_2 scattering) with the experimental ones. Model B was given by Henry and Lane,[28] the analytic form of $V_p^0(r)$ and $V_p^2(r)$ being determined by the least-squares fit to their[26] calculated polarization potential. In both models A and B we have used the same values for Q, α_0, and α_2 which are[14] $0.49e^2a_0^2$, $5.1786e^2a_0^3$, and $1.2019e^2a_0^3$, respectively.

With the use of Eqs. (2) and (3) the Glauber-type eikonal scattering amplitude for a fixed molecular orientation (θ_m,φ_m) can be obtained[20,21] in a convenient form. This amplitude then yields,[20,21] in the adiabatic approximation, the differential scattering cross sections [Eq. (6)] for the excitation process $J\to J'$ and average elastic differential scattering cross sections [Eq. (7)]:

$$I(J\to J',\theta)=\frac{k_i^2(2J'+1)}{4}\sum_{M=-J}^{J}\sum_{M'=-J}^{J'}\left|\left[\frac{(J-|M|)!}{(J+|M|)!}\frac{(J'-|M'|)!}{(J'+|M'|)!}\right]^{1/2}\right.$$
$$\left.\times P_J^{|M|}(\cos\theta_m)f_{2n,n}(\theta,\theta_m)P_{J'}^{|M'|}(\cos\theta_m)\sin\theta_m d\theta_m\right|^2 , \tag{6}$$

TABLE I. Total and momentum-transfer cross sections (in 10^{-20} m^2) for e^+-H_2 scattering (potential model A).

Energy (eV)	$\sigma(0\rightarrow 0)$	$\sigma(0\rightarrow 2)$ ($\times 10^{-2}$)	$\sigma(1\rightarrow 1)$	$\sigma(1\rightarrow 3)$ ($\times 10^{-2}$)	$\langle\sigma\rangle$	$\langle\sigma_m\rangle$
1.0	1.52	3.00	1.53	1.82	1.55	0.868
1.5	1.08	2.61	1.09	1.57	1.10	0.522
2.0	0.849	2.42	0.859	1.46	0.874	0.383
2.5	0.722	2.28	0.732	1.40	0.746	0.329
3.0	0.645	2.22	0.654	1.39	0.669	0.317
3.5	0.598	2.19	0.606	1.41	0.622	0.325
4.0	0.569	2.16	0.578	1.42	0.595	0.344
5.0	0.545	2.21	0.554	1.50	0.571	0.392
5.5	0.541	2.26	0.550	1.55	0.569	0.416
6.0	0.541	2.33	0.550	1.60	0.569	0.438
7.0	0.544	2.51	0.554	1.72	0.575	0.476
8.0	0.549	2.72	0.560	1.86	0.582	0.502
10.0	0.554	3.22	0.567	2.15	0.592	0.529
13.6	0.542	4.18	0.558	2.70	0.588	0.520
15	0.531	4.54	0.550	2.90	0.581	0.506
20	0.483	5.71	0.506	3.57	0.544	0.444
30	0.385	7.29	0.415	4.47	0.461	0.328
50	0.257	8.31	0.291	5.04	0.342	0.199
75	0.178	7.85	0.209	4.74	0.257	0.127
100	0.136	6.91	0.164	4.17	0.206	0.089
150	0.093	5.14	0.114	3.10	0.145	0.048

$$\langle I(\theta)\rangle=\frac{k_i^2}{2}\sum_{n=0}\int\lambda_n f_{2n,n}^2(\theta,\theta_m)\sin\theta_m d\theta_m\ , \tag{7}$$

with

$$\lambda_n=\begin{cases}1, & n=0\\ 2, & n\neq 0\end{cases}$$

$$2n=|M-M'|\ ,$$

where θ is the scattering angle, the P_J^M's are the associated Legendre polynomials, and k_i is the incident momentum. The $f_{2n,n}$'s are defined elsewhere.[21] Total cross sections $\sigma(J\rightarrow J')$ for the transition $J\rightarrow J'$ or the average total (elastic) cross sections $\langle\sigma\rangle$ are computed by using Eq. (6) or (7) in

$$\sigma=2\pi\int_0^\pi I(\theta)\sin\theta\, d\theta\ . \tag{8}$$

$\langle I(\theta)\rangle$ and $\langle\sigma\rangle$ include all the possible final rotational states for any initial rotational states J of the molecule. The numerical procedure used by us to compute the cross sections [Eqs. (6)–(8)] has been described elsewhere.[22]

III. RESULTS AND DISCUSSIONS

We have computed pure elastic-scattering ($J=0\rightarrow J'=0$ and $J=1\rightarrow J'=1$), pure rotational-excitation ($J=0\rightarrow J'=2$ and $J=1\rightarrow J'=3$), and orientationally averaged elastic-scattering cross sections using potential models A and B for incident positron energies of 1–200 eV. Both differential and total scattering cross sections are obtained. Momentum-transfer cross sections are also calculated in the same energy interval.

A. Positron scattering at low energies

Different total cross sections and the momentum-transfer cross sections $\langle\sigma_m\rangle$ obtained by using potential models A and B are presented in Tables I and II, respectively, to show their relative magnitudes. In Fig. 1 we have compared the present averaged total elastic- (elastic plus rotational) scattering cross sections at energies of 1–20 eV with those of other theoretical workers[14,16] and with the experimental total (elastic plus all possible inelastic) scattering cross sections measured by Coleman *et al.*[29] and Hoffman *et al.*[11] The results of Baille *et al.*[14] shown were calculated with a model potential exactly identical with our potential model B. We have plotted the one-center calculations of Darewych *et al.*[16] (a two-center version of which was reported earlier by Hara[15]) in which static potentials derived by using Kolos and Roothaan's wave function[30] and the adiabatic polarization potential of Hara[26] were used. Below the positronium formation threshold (8.63 eV), the present potential model B cross sections are found to give the best fit, compared to all other theoretical calculations including those of Sur and Ghosh[18] (not shown), to experimental measurements. In fact, these cross sections reproduce correctly the energy dependence of the measured cross sections of Hoffman *et al.*,[11] their magnitudes within experimental error (see, Table II), and even the observed minimum (at ~ 5 eV). Potential model A cross sections are smaller in magnitude, but their energy dependence resembles that of potential model B cross sections; the minimum occurs at about 5.5 eV. Potential model B calculations of Baille *et al.* lie below the present results for both the models, but show a

TABLE II. Total and momentum-transfer cross sections (in 10^{-20} m^2) for e^+-H_2 scattering (potential model B).

Energy (eV)	$\sigma(0\rightarrow 0)$	$\sigma(0\rightarrow 2)$ ($\times 10^{-2}$)	$\sigma(1\rightarrow 1)$	$\sigma(1\rightarrow 3)$ ($\times 10^{-2}$)	$\langle\sigma\rangle$	σ_T[a]	$\langle\sigma_m\rangle$
1.0	2.07	3.76	2.08	2.26	2.11	2.2 ±0.4	1.25
1.5	1.46	3.63	1.47	2.19	1.49	1.40±0.15	0.764
2.0	1.14	3.57	1.16	2.17	1.18	0.94±0.12	0.554
2.5	0.971	3.53	0.986	2.14	1.01		0.470
3.0	0.874	3.54	0.888	2.16	0.991	0.95±0.09	0.446
3.5	0.817	3.56	0.831	2.19	0.855		0.453
4.0	0.785	3.57	0.800	2.22	0.824	0.77±0.07	0.477
4.5	0.770	3.63	0.784	2.27	0.809		0.509
5.0	0.765	3.66	0.780	2.31	0.805	0.84±0.08	0.545
5.5	0.767	3.71	0.782	2.36	0.808		0.582
6.0	0.773	3.78	0.788	2.41	0.815	0.79±0.07	0.613
6.5	0.782	3.85	0.797	2.46	0.824		0.651
7.0	0.792	3.93	0.808	2.52	0.835	0.88±0.08	0.681
8.0	0.812	4.11	0.829	2.64	0.858	0.91±0.07	0.731
10.0	0.845	4.53	0.863	2.90	0.894	1.40±0.10	0.791
13.6	0.860	5.33	0.882	3.37	0.918		0.803
15	0.854	5.62	0.877	3.54	0.914		0.788
20	0.802	6.57	0.829	4.08	0.871		0.696
30	0.662	7.79	0.693	4.77	0.742		0.502
50	0.455	8.44	0.489	5.11	0.541		0.280
75	0.320	7.89	0.351	4.76	0.399		0.165
100	0.246	6.96	0.274	4.20	0.316		0.111
150	0.168	5.19	0.189	3.13	0.221		0.059
200	0.128	3.94	0.144	2.37	0.168		0.035

[a]Experimental, Hoffman *et al.* (Ref. 11).

striking similarity in energy dependence. The results of Darewych *et al.* are akin to experimental measurements between 2–7 eV with a different energy dependence. For both the models, the cross sections computed earlier by Bhattacharyya and Ghosh[17] (not shown) are higher than the corresponding ones obtained by the present method.

The rotational-excitation cross sections $\sigma(0\rightarrow 2)$ were calculated by several workers.[12,14–16] In Fig. 1 the present $\sigma(0\rightarrow 2)$ for potential model B at 1–20 eV are compared only with those reported by Darewych *et al.*[16] At lower energies present cross sections are about three to four times smaller but indicate a sharper increase in energy. No previous calculations for $\sigma(1\rightarrow 1)$ and $\sigma(1\rightarrow 3)$ are available. As is evident from Table II, the pure elastic cross sections $\sigma(J\rightarrow J)$ and rotational-excitation cross sections $\sigma(J\rightarrow J+2)$ depend upon the initial state J. At a particular energy, $\sigma(J\rightarrow J)$ increases and $\sigma(J\rightarrow J+2)$ decreases with the increase in J, while $\langle\sigma\rangle\simeq\sigma(J\rightarrow J)+\sigma(J\rightarrow J+2)$ remains insensitive to initial state J; this is in accordance with the standard results of the adiabatic-nuclei approximation, namely, the cross section for $J\rightarrow J'$ transitions summed over J' is independent of J. This result also shows that the contribution of $\sigma(J\rightarrow J')$ for $J'>J+2$, which depends mainly on the nonspherical potential represented by V^ν with $\nu>2$, to $\langle\sigma\rangle$ is almost negligible and thus justifies the truncation of the one-center expansion (2) at $\nu=2$ describing the positron–hydrogen-molecule potential. All these observations are also true for model A cross sections which are, however, smaller in magnitude (Table I).

In Fig. 2, differential scattering cross sections $\langle I(\theta)\rangle$ at some selected energies (1.5, 5.0, and 13.6 eV) and $I(0\rightarrow 2,\theta)$ at 13.6 eV for potential model B are presented. The angular dependence of these cross sections is not exactly similar to that of the corresponding cross sections (at and around the relevant energies) obtained by other workers[14–16,18] (not shown). The momentum-transfer cross sections $\langle\sigma_m\rangle$ as a function of incident momentum, however, show striking similarity in shape with those calculated by Baille *et al.*[14] and Darewych *et al.*[16] (Fig. 3).

As is evident from the above discussions the Glauber-type eikonal approximation, valid most at high and intermediate energies, explains adequately the scattering of low-energy positrons by the hydrogen molecule below the threshold for positronium formation. A possible explanation of it is given in Sec. III B 3. In this respect we would like to point out that Saha *et al.*[31] also observed that total cross sections for e^+-He scattering, obtained through the eikonal approximation, give a reasonable fit to experimental observations below the threshold for positronium formation. To our knowledge, no previous Glauber calculation of the rotational-excitation cross sections for low-energy positron-molecule scattering exists, but such a calculation is made earlier by Ashihara *et al.*[32] for electron-molecule scattering.

Above the positronium formation threshold, the experimental total cross sections increase sharply indicating the marked influence of the positronium formation channel.

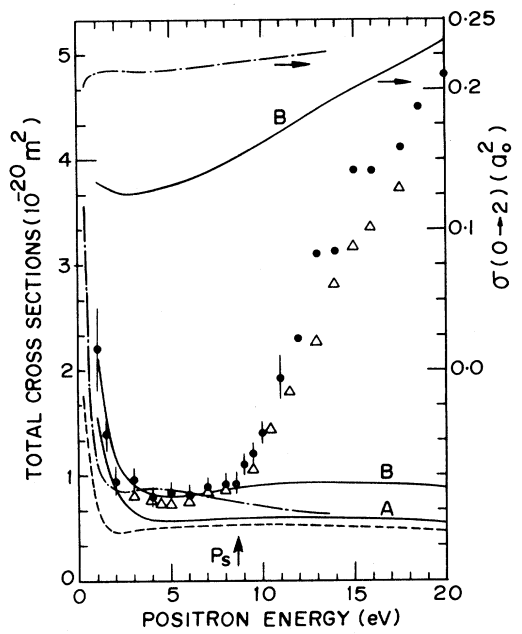

FIG. 1. Left-hand-side ordinate: comparison of theoretical average total elastic (elastic plus rotation) scattering cross sections with experimental total (elastic plus all possible inelastic) scattering cross sections for e^+-H_2 scattering at 1–20 eV. Theoretical: ——, present calculations with potential models A (curve *A*) and B (curve *B*); — — —, Baille *et al.* (the potential model is exactly the same as potential model B, Ref. 14); —·—·—, one-center calculations of Darewych *et al.* (Ref. 16). Experimental: △, Coleman *et al.* (Ref. 29); ●, Hoffman *et al.* (Ref. 11). Right-hand-side ordinate: comparison of total rotational-excitation cross sections $\sigma(0\rightarrow2)$. ——, present calculations with model B (curve *B*); —·—·—, one-center calculations of Darewych *et al.* (Ref. 16).

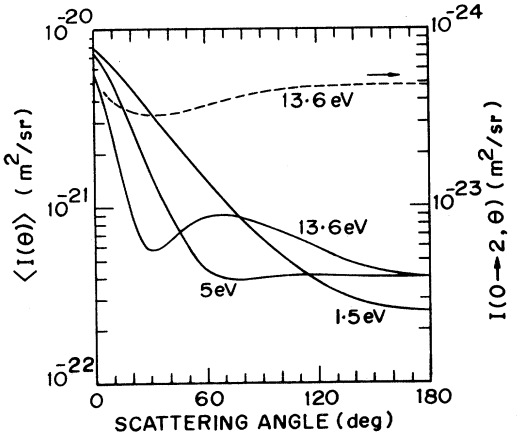

FIG. 2. Left-hand-side ordinate: present average elastic differential scattering cross sections (potential model B) for e^+-H_2 scattering at 1.5, 5.0, and 13.6 eV. Right-hand-side ordinate: state-to-state differential scattering cross sections for the process $J=0\rightarrow J'=2$ at 13.6 eV (model B).

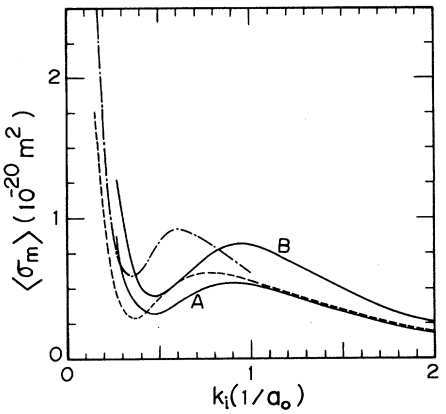

FIG. 3. Momentum-transfer cross sections for e^+-H_2 scattering as a function of incident momentum. ——, present calculations with potential models A (curve *A*), and B (curve *B*); — — —, Baille *et al.* (same as model B, Ref. 14); —·—·—, one-center calculations of Darewych *et al.* (Ref. 16).

Recently, Charlton *et al.*[33] have observed a peak near the ionization threshold (15.6 eV) in the energy dependence of the orthopositronium formation cross sections for hydrogen molecule. The increase in experimental total cross sections still beyond the ionization threshold suggests that appreciable contribution to total cross sections comes from inelastic channels other than the positronium forma-

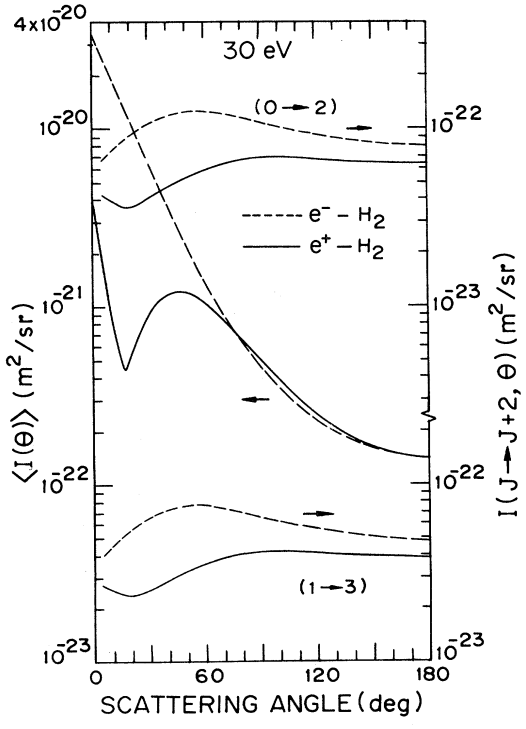

FIG. 4. Comparison of average elastic and state-to-state rotational-excitation differential scattering cross sections for positron— and electron—hydrogen-molecule scattering at 30 eV using potential model B. ——, positron; — — —, electron (Ref. 21). (Arrows indicate which scales apply.)

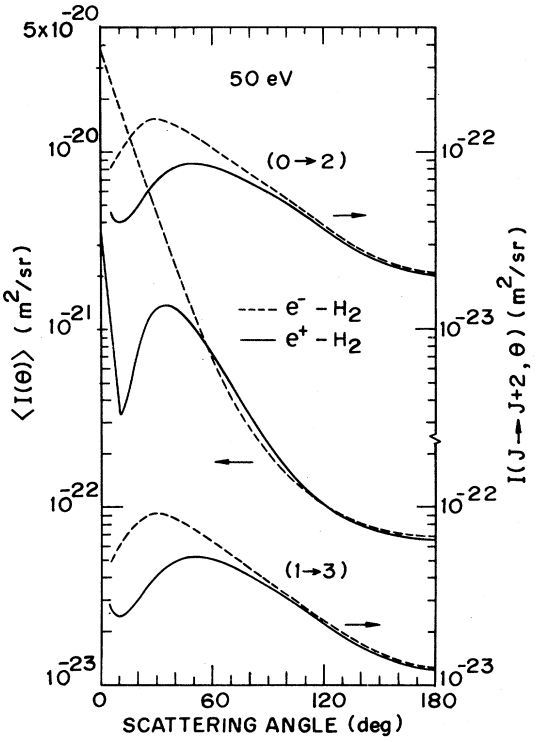

FIG. 5. Same as Fig. 4, but for incident energy 50 eV.

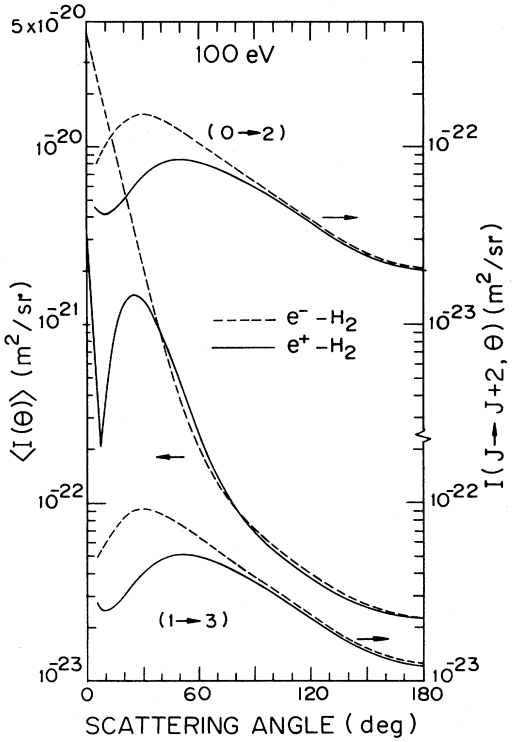

FIG. 6. Same as Fig. 4, but for incident energy 100 eV.

tion one beyond this energy. A suitable effective local absorption potential, which is neglected in the present investigation, might explain, to some extent, the rise in observed total cross sections above the positronium formation threshold.

B. Comparison of positron and electron scattering at intermediate energies

Average elastic and state-to-state differential scattering cross sections for positron scattering at energies of 30, 50, and 100 eV obtained by using potential model B are presented in Figs. 4—6, respectively. These cross sections at 50 eV are given in Table III. In our earlier studies[21—23] we observed that the present method is successful in explaining the electron-molecule scattering at intermediate energies, roughly characterized as impact energies from ionization potential to ten times the ionization potential. It fails at low energies, roughly around and below the ionization potential of the molecule. As such, it is the intermediate-energy region where a comparison of electron and positron cross sections, both differential and total, obtained by the present method is of much interest. Such a comparison, particularly of the differential scattering cross sections for different processes and their energy dependence, is expected to provide useful insight into the role of positrons and electrons as projectiles. In Figs. 4—6 we have also made this comparison of the differential scattering cross sections (model B) for the molecular target hydrogen. Cross sections for electron scattering without exchange at pertinent energies were computed earlier by Bhattacharyya *et al.*[21]

At each energy marked differences in the cross sections for the two projectiles are found to occur only at lower scattering angles. With the increase in scattering angle $\langle I(\theta)\rangle$ curve for positrons passes through a minimum and a maximum at angles θ_1 and θ_2, respectively, but that for electrons decreases smoothly; the two curves then cross each other for the first time at an angle θ_3. Within the angular region $0°$—θ_3 the positron cross sections are considerably smaller in magnitude, they become comparable with electrons cross sections above the scattering angle θ_3. The angles θ_1, θ_2, and θ_3 decrease with the increase in energy so that the angular region $0°$—θ_3 shortens towards the forward direction. These angles and the corresponding cross sections for a few incident energies are given in Table IV.

At a particular energy $I(J\rightarrow J+2,\theta)$ for positrons lies below that for electrons at all scattering angles. But now the angular region where they differ appreciably extends slightly beyond θ_3. Within this angular region electron cross sections show a broad maximum in between the narrow minimum and the broad maximum exhibited by positron cross sections. The maximum for positrons occurs nearer to θ_3. The energy dependence of this angular region resembles that for $\langle I(\theta)\rangle$. The characteristic features of pure elastic cross sections $I(J\rightarrow J,\theta)$ are similar to those for $\langle I(\theta)\rangle$ (for 50 eV, see Table III for positrons and Table III in Ref. 21 for electrons).

In the energy interval 20—200 eV where calculations are

TABLE III. Average elastic and state-to-state differential scattering cross sections (in 10^{-22} m^2/sr) for positron-H_2 scattering (potential model B) at 50 eV.

θ (deg)	$I(0\rightarrow0)$	$I(0\rightarrow2)$	$I(1\rightarrow1)$	$I(1\rightarrow3)$	$\langle I(\theta)\rangle$
0	36.33		36.34		36.41
5	11.59	0.464	11.78	0.287	12.07
10	3.311	0.407	3.474	0.252	3.737
15	3.967	0.395	4.125	0.245	4.380
20	7.416	0.412	7.580	0.255	7.845
25	10.67	0.448	10.85	0.276	11.13
30	12.63	0.497	12.83	0.305	13.14
35	13.18	0.551	13.40	0.338	13.74
40	12.63	0.606	12.87	0.370	13.25
50	9.839	0.703	10.12	0.427	10.56
60	6.677	0.756	6.980	0.459	7.445
70	4.195	0.776	4.505	0.470	4.981
80	2.541	0.774	2.851	0.468	3.324
90	1.521	0.752	1.822	0.455	2.282
100	0.920	0.723	1.209	0.437	1.650
110	0.572	0.692	0.848	0.418	1.270
120	0.370	0.661	0.634	0.399	1.037
130	0.251	0.631	0.504	0.381	0.888
140	0.181	0.606	0.424	0.366	0.793
150	0.140	0.586	0.374	0.354	0.731
160	0.116	0.571	0.345	0.345	0.693
170	0.104	0.560	0.328	0.339	0.670
180	0.100	0.557	0.323	0.337	0.663

made for both positrons and electrons total cross sections $\langle\sigma\rangle$ for positrons (Table II) are considerably smaller than those for electrons (Table IV, Ref. 21). This is because the major contribution to $\langle\sigma\rangle$ comes from scattering at small angles and positron cross sections are significantly smaller in magnitude at these angles.

1. Effects of the spherical part of the potential

The characteristics of the angular distribution of different cross sections for positrons (electrons) can be qualitatively explained by studying separately the effects of various contributions to static and polarization potentials

TABLE IV. Characteristic scattering angles (in deg) and the corresponding differential scattering cross sections (in 10^{-22} m^2/sr) for positron scattering (potential model B).

Energy (eV)	Potential (model B)	θ_1[a]	θ_2[b]	θ_3[c]	θ_4[d]	$\langle I(\theta_1)\rangle$	$\langle I(\theta_2)\rangle$	$\langle I(\theta_3)\rangle$	$\langle I(\theta_4)\rangle$ ($\times10^{-3}$)
5	V^0	70	120			5.744	6.498		
30	V	16.5	45	75		4.478	12.34	7.574	
	V^0	15	45	71		2.973	13.51	8.960	
	V_p^0				69				1.789
50	V	11.5	35	55.5		3.336	13.75	8.793	
	V^0	11	35	52		1.947	14.31	10.05	
	V_p^0				52				1.087
100	V	7.5	25	38		2.092	14.92	9.872	
	V^0	7.5	25	36		1.048	14.92	10.60	
	V_p^0				36				0.616
200	V	5	17	26.5		1.344	15.53	10.43	
	V^0	5	17	25		0.536	15.24	11.04	
	V_p^0				25				0.879

[a]Minimum in positron cross sections occurs at this angle.
[b]Maximum in positron cross sections occurs at this angle.
[c]Electron and positron cross sections become identical at this angle.
[d]Minimum in V_p^0 cross sections occurs at this angle.

TABLE V. Spherical potentials (model B) for $e^{\pm}$-H_2 scattering in Hartree atomic units.

r (a_0)	$V_s^0(e^-)$	$V_p^0(e^{\pm})$	$V^0(e^-)$	$V^0(e^+)$
0.0	−1.014	0.000	−1.014	1.014
0.2	−1.031	-1.803^{-3}[a]	−1.033	1.029
0.4	−1.080	-1.233^{-2}	−1.092	1.067
0.6	−1.159	-3.260^{-2}	−1.191	1.126
0.7	−1.208	-4.461^{-2}	−1.253	1.163
0.8	-9.051^{-1}	-5.657^{-2}	-9.617^{-1}	8.486^{-1}
1.0	-5.224^{-1}	-7.701^{-2}	-5.995^{-1}	4.454^{-1}
1.2	-3.088^{-1}	-8.953^{-2}	-3.983^{-1}	2.192^{-1}
1.3	-2.388^{-1}	-9.242^{-2}	-3.312^{-1}	1.464^{-1}
1.4	-1.852^{-1}	-9.318^{-2}	-2.784^{-1}	9.201^{-2}
1.5	-1.440^{-1}	-9.206^{-2}	-2.360^{-1}	5.192^{-2}
1.6	-1.122^{-1}	-8.935^{-2}	-2.015^{-1}	2.282^{-2}
1.7	-8.754^{-2}	-8.538^{-2}	-1.729^{-1}	2.159^{-3}
1.8	-6.841^{-2}	-8.048^{-2}	-1.489^{-1}	-1.206^{-2}
2.0	-4.194^{-2}	-6.909^{-2}	-1.110^{-1}	-2.715^{-2}
2.2	-2.580^{-2}	-5.725^{-2}	-8.305^{-2}	-3.145^{-2}
2.5	-1.252^{-2}	-4.144^{-2}	-5.396^{-2}	-2.892^{-2}
3.0	-3.787^{-3}	-2.344^{-2}	-2.723^{-2}	-1.965^{-2}
5.0	-3.356^{-5}	-3.690^{-3}	-3.724^{-3}	-3.657^{-3}

[a]Numbers a^n stand for $a \times 10^n$.

and also those of the spherical and nonspherical parts (with the appropriate combination of the corresponding static and polarization potentials) of the effective positron(electron)-molecule potential. In Table V we have given model B spherical potentials used in the present calculations and the corresponding differential scattering cross sections at 30 and 50 eV are displayed in Figs. 7 and 8, respectively. A comparison of positron cross sections presented in Figs. 7 and 8 with those in Figs. 4 and 5 reveals that the shape of average elastic differential scattering cross sections is primarily determined by the spherical part of the potential (V^0). The characteristic angles θ_1, θ_2, and θ_3 for positrons obtained in the case of the spherical potential V^0 alone are almost identical with those determined by using the complete potential V given by Eqs. (2) and (3) (Table IV).

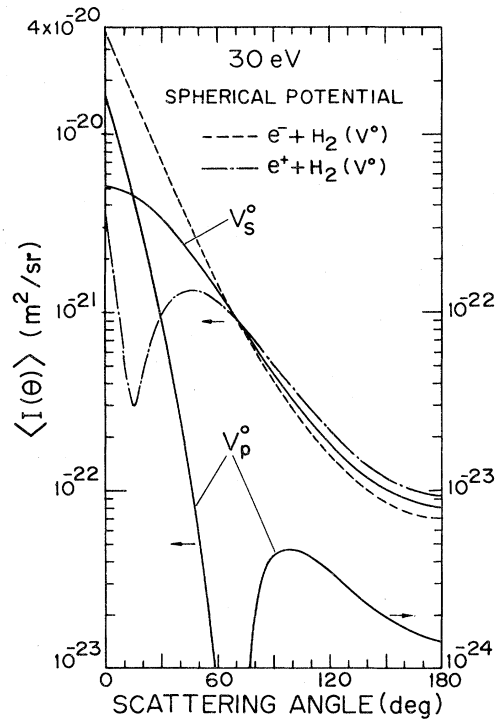

FIG. 7. Comparison of elastic differential scattering cross sections obtained by using the spherical part V^0 of potential model B for $e^{\pm}$-H_2 scattering at 30 eV. Elastic differential scattering cross sections due to scattering by short-range static potential V_s^0 and long-range polarization potential V_p^0 alone are also shown. Note that the tail of V_p^0 curve is plotted in a different scale as indicated by arrow.

Figures 7 and 8 show[34] that cross sections for the short-range spherical potential V_s^0 are appreciable over a wider range of scattering angles than those for the long-range potential V_p^0. V_p^0 cross sections exhibit steeper rise at small scattering angles and pass through a very sharp minimum[34] at an angle θ_4 which decreases with increasing energy (Table IV). This angle corresponds to the angle θ_3 (V^0) where the scattering is determined by V_s^0 alone and the two projectiles become indistinguishable. For positrons effects of static and polarization potentials are constructive above the angle θ_3, but they are destructive below it; the situation reverses in the case of electrons. Because of the extremely small effects of polarization above the scattering angle θ_3 positron and electron cross sections in this region lie symmetrically above and below V_s^0 cross sections and are comparable with each other. Below the scattering angle θ_3 the effects of polarization become increasingly dominant as one moves towards the forward direction. Since the effects of static and polarization potentials are destructive for positrons in this region, positron cross sections give rise to a maximum at θ_2 and a miminum at θ_1; the position of the minimum coincides with the angle where the cross sections for V_s^0 and V_p^0 become equal. For electrons, on the other hand, these effects are in phase and the cross sections rise steadily below the angle θ_3.

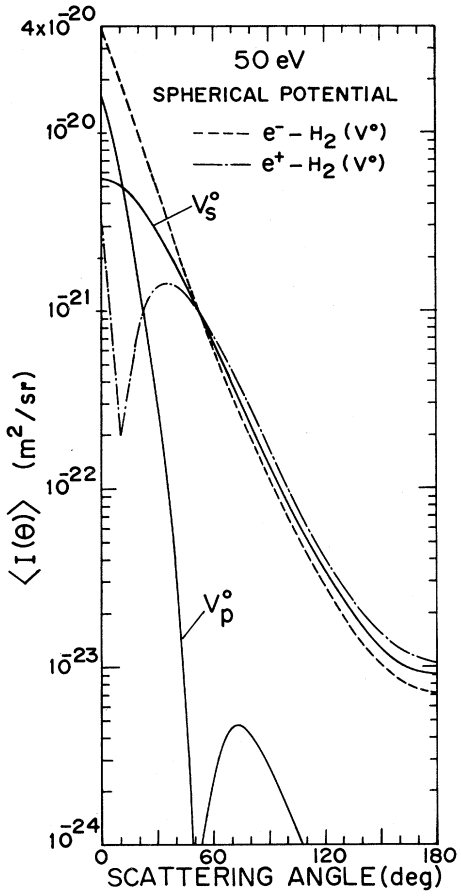

FIG. 8. Same as Fig. 7, but for incident energy 50 eV.

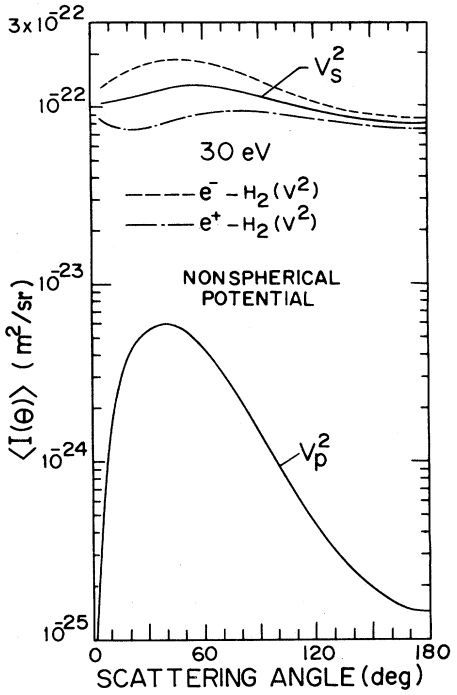

FIG. 9. Comparison of average elastic differential scattering cross sections obtained by using the nonspherical part V^2 of potential model B for $e^{\pm}$-H_2 scattering at 30 eV. Elastic differential scattering cross sections due to scattering by nonspherical static potential V_s^2 and polarization potential V_p^2 alone are also shown.

2. Effects of nonspherical part of the potential

Our results[34] for the nonspherical part of the potential (model B) at 30 and 50 eV are shown in Figs. 9 and 10, respectively. The static potential V_s^2 is found to dominate over the polarization potential V_p^2. Cross sections due to V_s^2, although they show a broad maximum (at 50 eV it occurs at 50°), are almost independent of scattering angle. Cross sections due to V_p^2, on the other hand, exhibit a sharp maximum (at 50 eV it occurs at 30°) and fall more rapidly at lower angles than at larger angles. These maxima shift towards the forward direction as the energy increases. The appropriate combination of V_s^2 and V_p^2 results in the cross sections for positrons and electrons, as shown in Figs. 9 and 10, due to the nonspherical potential V^2 alone. Since the rotational excitation is caused by the nonspherical potential the angular variation of these cross sections resembles that of $I(J\rightarrow J+2,\theta)$ for the pertinent projectile (Figs. 5 and 6). Inclusion of V^2 slightly changes the scattering angle θ_3 obtained by using V^0 (Table IV). The effects of the nonspherical potential are small below θ_3, but become prominent roughly from and above the scattering angle θ_3.

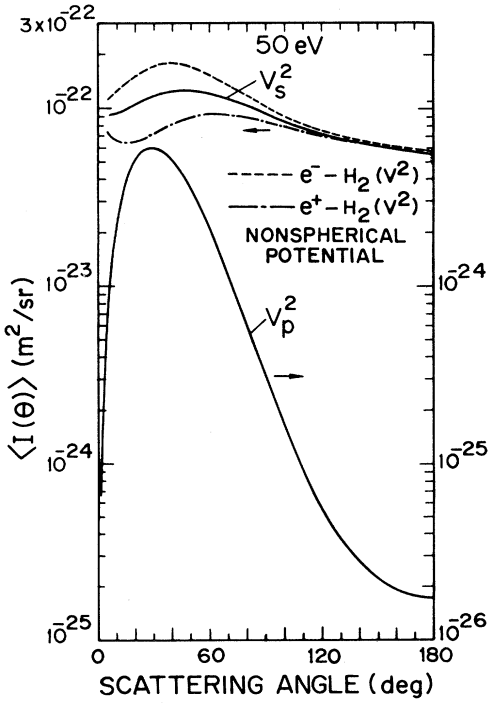

FIG. 10. Same as Fig. 9, but for incident energy 50 eV. (Arrows indicate which scales apply.)

TABLE VI. Comparison of total inelastic scattering cross sections $\sigma_{in}=\sigma_T{}^a-\langle\sigma\rangle^b$ for e^+-H_2 and e^--H_2 scattering (in 10^{-20} m^2).

Energy (eV)	Positron		Electron	
	Model A	Model B	Model A	Model B
30	4.41	4.13	2.48	2.74
40	4.05	3.81	2.26	2.52
50	3.67	3.47	1.91	2.16
75	2.99	2.85	1.65	1.84
100	2.47	2.36	1.56	1.72
150			1.29	1.40
200		1.58	1.29	1.25

[a]Experimental total scattering cross sections, Hoffman *et al.* (Ref. 11).

[b]Theoretical total elastic scattering cross sections obtained by using the present method: positron scattering (present calculations); electron scattering (Bhattacharyya *et al.*, Ref. 21).

3. A few observations

In Figs. 7 and 8 we have shown that cross sections due to V_p^0 alone exhibit a sharp minimum. The position of this minimum, the scattering angle θ_4, is correlated[34] with the position of the minimum in V_p^0 at $r=1.4a_0$ (see column 3 in Table V). The angle θ_4 is almost identical with θ_3 which has the property that the scattering at this angle does not discriminate between the two projectiles. The scattering cross section here is determined by the static potential V_s^0 alone. This is because V_p^0 cross sections are about 10^3 times smaller than V_s^0 cross sections at $\theta\simeq\theta_4$ and the nonspherical potential V^2 is very weak for the hydrogen molecule. Thus the positron scattering at the angle $\theta=\theta_3$ might be correlated with the positron-H_2 potential at $r\simeq 1.4a_0$. The scattering within the angular region 0^0—θ_3 is largely governed by the positron-H_2 potential effective in the region of space $r\geq 1.4a_0$. The cancellation of polarization and static potentials that occurs roughly between $r=1.4a_0$ and $r=5a_0$ is reflected in the shape of the average differential scattering cross sections for positrons within this anglular region and the positions of the maximum (θ_2) and minimum (θ_1) depend upon the degree of cancellation of these potentials. Maximum cancellation takes place at $r=2.2a_0$ (see column 5, Table V) which causes $\langle I(\theta)\rangle$ for positrons to have a minimum at θ_1.

As discussed above, knowledge of the scattering angles θ_1, θ_2, and θ_3 has important bearing on our understanding of the positron(electron)-molecule potential. For the hydrogen molecule, these angles are determined primarily by the spherical part of the potential. This might not be true for a molecular target with a stronger nonspherical potential V^2, such as nitrogen or oxygen. In any case, reliable information regarding the accuracy of static and polarization potentials and their degree of cancellation could be derived by carefully comparing the computed values of the angles θ_1, θ_2, and θ_3 with those obtained experimentally. Unfortunately, experimental determination of average elastic differential scattering cross sections for positrons has not yet to become a reality.

The fact that the scattering within the angular region $0°$—θ_3 is correlated with the potential in the region of space $r\geq 1.4a_0$ provides a possible explanation of the validity of the present method only in the case of low-energy positron scattering. At 5 eV, for example, we observe that V_p^0 cross sections do not display a minimum and the angular region $0°$—θ_3 apparently covers the entire scattering region $0°$—$180°$ (see Table IV and Fig. 2). This suggests that the potential in the region of space for which $r\geq 1.4a_0$ is most effective for scattering throughout the scattering angles at this energy. In this region of space, as is evident from Table V, the high-energy approximation $V(r)/E<1$, where E is the incident energy, is satisfied for positrons if one considers the spherical potential $V^0(r)$ for $V(r)$. For electrons, on the other hand, this condition fails at $r=1.4a_0$ and over a considerable range above it.

At an energy as high as 200 eV, the angle θ_3, which is the measure of up to what extent the polarization is important, is about 25° and the average total elastic cross sections for positron scattering (0.168×10^{-20} m^2, Table II) is about 2.5 times smaller than that for electron scattering without exchange (0.443×10^{-20} m^2, Table IV, Ref. 21) for potential model B. This shows that the polarization interaction is appreciable enough to distinguish the two projecties even at 200 eV. Hoffman *et al.*[11] measured, in the same apparatus, total scattering cross sections for e^+-H_2 and e^--H_2 scattering. They observed, contrary to expectation, that electron results are lower than positron results in the energy region 30—200 eV; they become identical (to within 2%) at and above 200 eV. They inferred that the contribution of inelastic cross sections to total cross sections for positrons considerably exceeds that for electrons between 30—200 eV. An estimate and comparison of this contribution (σ_{in}) for the two projectiles can be made by utilizing total elastic cross sections $\langle\sigma\rangle$ obtained by using the present method for electrons (without exchange)[21] and positrons (present calculations) and the corresponding experimental total cross sections σ_T of Hoffman *et al.* in the expression $\sigma_{in}=\sigma_T-\langle\sigma\rangle$. This is shown in Table VI. As is evident from Table VI, σ_{in} for positrons dominates over that for electrons up to the highest incident energy (200 eV, model B) studied. It is likely that this dominance continues, as the large difference in total average elastic cross sections for the two projectiles suggests, even beyond this energy.

IV. SUMMARY AND CONCLUSIONS

Positron scattering by molecular hydrogen at incident energies 1—200 eV covering low- and intermediate-energy regions is studied, for the first time, by employing the same approximation, the Glauber-type eikonal approximation. Two forms of model effective potentials, both comprising only static and polarization potentials but differing in the form of the latter, are used. Of these, the potential model B is found to reproduce accurately, below the positronium formation threshold, the energy dependence of the measured total cross sections of Hoffman *et al.*,[11] their magnitude within experimental error, and even the position of the minimum at 5 eV. Model A cross sections are only somewhat smaller in magnitude.

A detail comparison of positron and electron scattering

at intermediate energies is made. The effects of different terms and the spherical and nonspherical parts of potential model B on cross sections are examined to ascertain in which energy and angular region each is important. Calculations show that for average elastic differential scattering cross sections the influence of polarization is mainly confined within the angular region $0°-\theta_3$, where θ_3 is approximately the position of the minimum in V_p^0 cross sections. The characteristics of angular distribution of cross sections within this angular region is correlated with the nature of potential in the region of space for which $r \geq 1.4a_0$. Due to cancellation of static and polarization potentials that results in the positron case roughly in the region of space $1.4a_0 \leq r \leq 5a_0$ the positron cross sections within $0°-\theta_3$ become considerably smaller than electron cross sections and show a maximum and minimum. The position of the minimum is correlated with the minimum in the potential at $r = 2.2a_0$ where maximum cancellation takes place. With the increase in energy the region $0°-\theta_3$ decreases towards the forward direction. At the highest energy investigated $\theta_3 = 25°$ which shows that the effects of polarization is quite appreciable to distinguish the two projectiles.

We have pointed out that the appreciable reduction in the strength of the potential in the region of space most effective for scattering at low energies makes the present approximation suitable for positron-H_2 scattering at such energies. Further investigation on molecular targets possessing a stronger static potential is needed to learn more about its applicability to low-energy positron scattering in general. In the present investigation effects of exchange for electron scattering, and those of positronium formation in case of positron scattering have been neglected. A comparitive study which includes these effects might provide better insight into the role of electrons and positrons as projectiles.

[1]H. S. W. Massey, Can. J. Phys. 60, 461 (1982).

[2]P. G. Coleman, T. C. Griffith, G. R. Heyland, and T. L. Killeen, in *Atomic Physics,* edited by G. zu Putlitz, E. W. Weber, and A. Winnacker (Plenum, New York, 1975), Vol. 4, p. 355.

[3]T. C. Griffith and G. R. Heyland, Phys. Rep. 39C, 169 (1978).

[4]T. C. Griffith, in *Advances in Atomic and Molecular Physics,* edited by D. R. Bates and B. Bederson (Academic, New York, 1979), Vol. 15, p. 134.

[5]W. E. Kauppila and T. S. Stein, Can. J. Phys. 60, 471 (1982).

[6]J. W. Humberston, in *Advances in Atomic and Molecular Physics,* edited by D. R. Bates and B. Bederson (Academic, New York, 1979), Vol. 15, p. 101.

[7]A. S. Ghosh, N. C. Sil, and P. Mondal, Phys. Rep. 87, 313 (1982).

[8]D. M. Schrader and R. E. Svetic, Can. J. Phys. 60, 517 (1982).

[9]M. Charlton, T. C. Griffith, G. R. Heyland, and T. R. Twomey, J. Phys. B 13, L239 (1980); W. E. Kauppila, T. S. Stein, J. H. Smart, M. S. Debabneh, Y. K. Ho, J. P. Downing, and V. Pol, Phys. Rev. A 24, 725 (1981); M. S. Debabneh, Y. F. Hsieh, W. E. Kauppila, V. Pol, and T. S. Stein, *ibid.* 26, 1252 (1982).

[10]M. Charlton, T. C. Griffith, G. R. Heyland, and G. L. Wright, J. Phys. B 13, L353 (1980).

[11]K. R. Hoffman, M. S. Dababneh, Y. F. Hsieh, W. E. Kauppila, V. Pol, J. H. Smart, and T. S. Stein, Phys. Rev. A 25, 1393 (1982).

[12]S. Hara, J. Phys. B 5, 589 (1972) (H_2, N_2, and O_2); J. W. Darewych, *ibid.* 15, L415 (1982) (N_2) and references therein.

[13]J. G. Lodge, J. W. Darewych, and R. P. McEachran, Can. J. Phys. 49, 13 (1971); 51, 779(E) (1973).

[14]P. Baille, J. W. Darewych, and J. G. Lodge, Can. J. Phys. 54, 667 (1974).

[15]S. Hara, J. Phys. B 7, 1748 (1974).

[16]J. W. Darewych, P. Baille, and S. Hara, J. Phys. B 7, 2047 (1974).

[17]P. K. Bhattacharyya and A. S. Ghosh, Phys. Rev. A 12, 1881 (1975).

[18]S. Sur and A. S. Ghosh, Can. J. Phys. 60, 597 (1982).

[19]S. Hara, J. Phys. Soc. Jpn. 22, 710 (1967).

[20]P. K. Bhattacharyya and A. S. Ghosh, Phys. Rev. A 14, 1587 (1976).

[21]P. K. Bhattacharyya, K. K. Goswami, and A. S. Ghosh, Phys. Rev. A 18, 1865 (1978). H_2.

[22]P. K. Bhattacharyya and K. K. Goswami, Phys. Rev. A 26, 2592 (1982). N_2.

[23]P. K. Bhattacharyya and K. K. Goswami, Phys. Rev. A 28, 713 (1983). O_2.

[24]S. C. Wang, Phys. Rev. 31, 579 (1928).

[25]P. K. Bhattacharyya and A. S. Ghosh, Phys. Rev. A 12, 480 (1975). For erratum, see Ref. 2 cited in Ref. 21.

[26]For example, N. F. Lane and R. J. W. Henry, Phys. Rev. 173, 183 (1968); S. Hara, J. Phys. Soc. Jpn. 27, 1262 (1969) (e^--H_2); D. G. Truhlar and F. A. Van-Catledge, J. Chem. Phys. 69, 3575 (1978) (e^--N_2 and e^--CO); R. A. Eades, D. G. Truhlar, and D. A. Dixon, Phys. Rev. A 20, 867 and references therein (e^--N_2).

[27]D. G. Truhlar, K. Onda, R. A. Eades, and D. A. Dixon, Int. J. Quantum Chem. Symp. 13, 601 (1979).

[28]R. J. W. Henry and N. F. Lane, Phys. Rev. 183, 221 (1969).

[29]P. G. Coleman, T. C. Griffith, G. R. Heyland, and T. R. Twomey, as reported in Ref. 3.

[30]W. Kolos and C. C. Roothaan, Rev. Mod. Phys. 32, 219 (1960).

[31]B. C. Saha, K. Sarkar, and A. S. Ghosh, Proc. Indian Acad. Sci. Sect. A 39, 382 (1973).

[32]O. Ashihara, I. Shimamura, and K. Takayanagi, J. Phys. Soc. Jpn. 38, 1732 (1975).

[33]M. Charlton, T. C. Griffith, G. R. Heyland, K. S. Lines, and G. L. Wright, J. Phys. B 13, L757 (1980).

[34]The characteristics of the angular distributions for scattering by the various parts of the potential obtained by us are similar to those observed by Truhlar and Rice [J. Chem. Phys. 52, 4480 (1970); 55, 2005(E) (1971)] in their plane-wave calculations. For energies studied (Table IV) we observe that the minimum in V_s^0 cross sections, which correlates with the minimum in V_s^0, occurs at large angles for enregies ≥ 100 eV. At 100 eV, for example, this angle is 120°.